

# **Oxford Chemistry Primers: Foundations of Surface Science**

**Solutions for Chapter Five: Techniques**

**5.1. The  $\text{Ru}\{0001\}$  surface has a structure in which hexagonal close-packed planes of atoms alternate in the ...ABABAB... stacking sequence. Show explicitly that the LEED pattern in Fig. 5.2 is consistent with a  $p(2\times 2)$  overlayer, and explain why it displays six-fold rotational symmetry (in both spot position and intensity) when an idealised instance of the  $\text{Ru}\{0001\}$  surface conforms only to the  $p3m1$  space group.**

A good starting point for this solution will be to sketch the ideal version of the surface in question. We are told that each plane of atoms is close-packed in a hexagonal arrangement, and that planes alternate in their lateral position. Assuming that each plane nestles into the hollow sites of the layer below (we can confirm this by looking up the crystal structure of bulk ruthenium) we arrive at the structure shown in Fig. 1. The surface displays threefold rotational symmetry, and there are three distinct mirror symmetries. Comparison against the symmetry archetypes shown in Fig. 2.4 (Section 2.3) confirms that the space group of the ideal surface is  $p3m1$  as stated in the question.

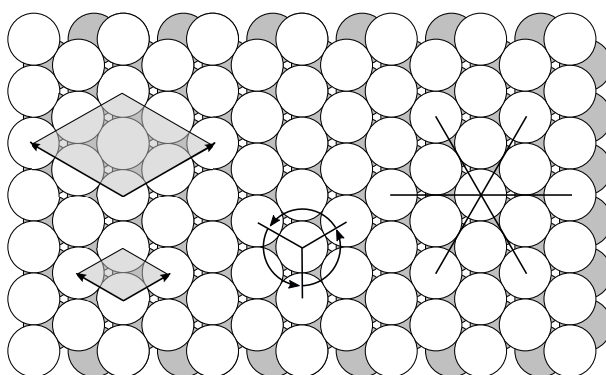


Figure 1: Schematic view of the  $\text{Ru}\{0001\}$  surface, with  $(1\times 1)$  and  $p(2\times 2)$  unit cells marked. Also indicated are a threefold rotational axis and three distinct mirror-plane orientations, consistent with the  $p3m1$  space group.

Our sketch makes clear that the two-dimensional real-space lattice of the ideal surface is triangular in nature, and we can therefore choose two primitive real-space lattice vectors, spanning the  $(1\times 1)$  unit cell, of equal length and separated by an angle of  $120^\circ$  (see Fig. 1). From this fact, and considering Eqn. 2.11 (Section 2.6) it follows that the two corresponding primitive reciprocal lattice vectors must also be of equal length (to one another, not to the real-space vectors) and that they are separated by an angle of  $60^\circ$ . The reciprocal lattice of the ideal surface is therefore triangular in nature, just like its real-space lattice (see Fig. 2.a & b).

As discussed in Section 5.2, the diffraction pattern obtained in a standard LEED experiment should match the reciprocal lattice of the surface. We therefore expect that the LEED pattern of the ideal surface would comprise a triangular lattice of diffraction spots, and this is indeed consistent with the arrangement of filled circles in Fig. 5.2, which we are told correspond to the clean surface.

If a  $p(2\times 2)$  overlayer were to be formed on the surface (see Fig. 1) then the real-space lattice would remain triangular in nature, but with primitive vectors doubled in length. Accordingly, the reciprocal lattice would also remain triangular in nature, but with primitive vectors halved in length (see Fig. 2.c & d). The LEED pattern would therefore comprise a triangular lattice of diffraction spots at half the spacing found for the clean surface. Evidently the diffraction spots observed for the clean surface would remain in the overlayer

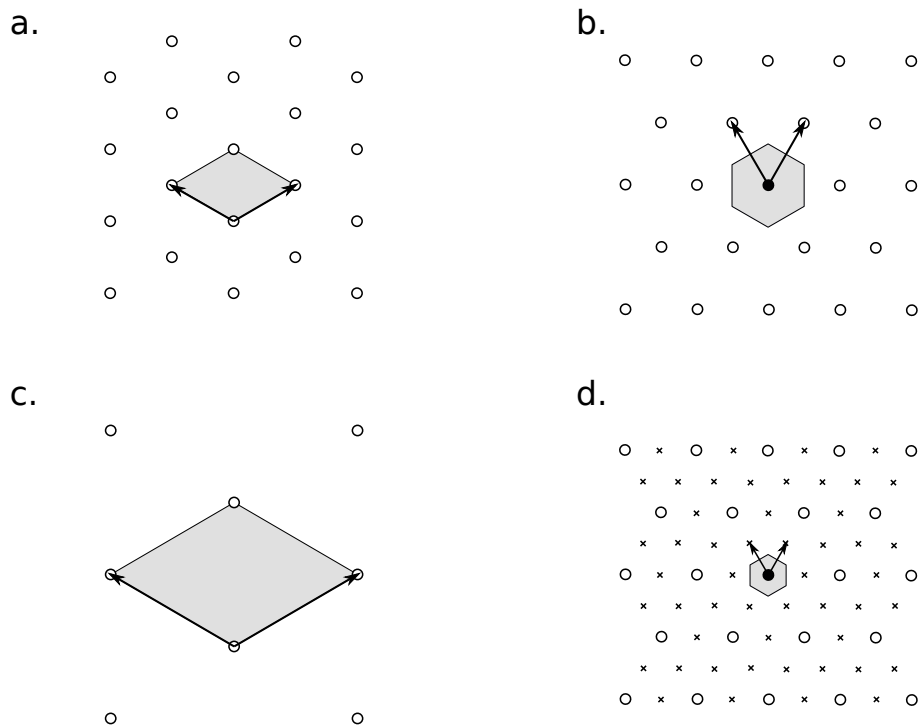


Figure 2: *Real-space and reciprocal lattices for  $Ru\{0001\}$ . In (a) we show the real-space lattice of the ideal surface, and in (b) the corresponding reciprocal lattice (which is also that surface's LEED pattern). In (c) we show the real-space lattice of the  $p(2 \times 2)$  surface, and in (d) the corresponding reciprocal lattice, with additional reciprocal lattice points (which imply additional LEED spots) marked as crosses.*

case, but additional spots would now also be present and would correspond to the crosses marked in Fig. 5.2.

In terms of the arrangement of diffraction spots in the LEED pattern, therefore, we have confirmed that the depiction in Fig. 5.2 is indeed consistent with a  $p(2 \times 2)$  superstructure. Such a pattern clearly displays six-fold rotational symmetry with respect to the location of the spots, but what about the spot intensities?

We know, from the discussion of LEED- $I/V$  experiments in Section 5.2, that spot intensities will generally vary as a function of the electron beam energy. Nevertheless, for any single specific energy the spot intensities ought to respect the symmetry of the surface. Addition of a  $p(2 \times 2)$  superstructure need not alter the  $p3m1$  space group of the surface, so long as the adsorbates occupy either hollow or atop sites, so in this case we can quite reasonably accept that the spot intensities might still display three-fold rotational symmetry and three distinct mirror symmetries. In Fig. 3.a, the spots have been marked to indicate groups that must share equivalent intensities by virtue of these symmetries. On the face of it, however, there would be no expectation of either six-fold rotational symmetry or more than three mirror symmetries, and yet the question tells us that such symmetries were actually observed in the experiment.

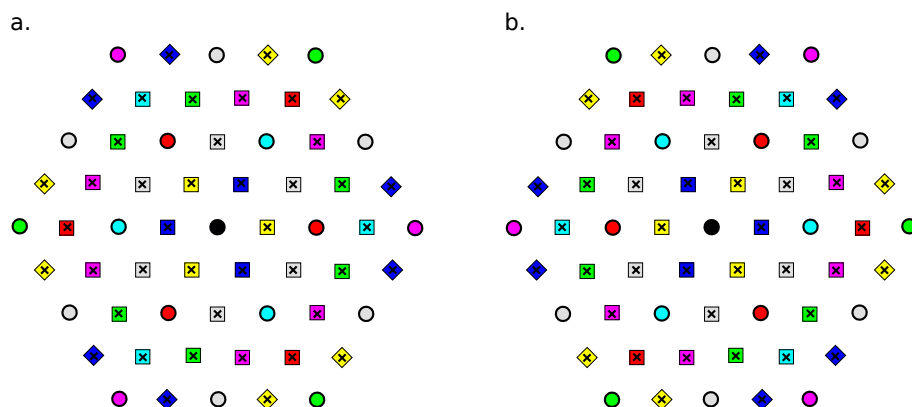


Figure 3: *Symmetry of spot intensities, consistent with the  $p3m1$  space group. In (a) the spots are marked with different shapes and colours to indicate those that must have identical intensities, assuming diffraction to arise from a single-terrace domain. In (b) the pattern of intensities is marked for a domain comprising a single terrace offset in height from the first by an odd number of atomic layers.*

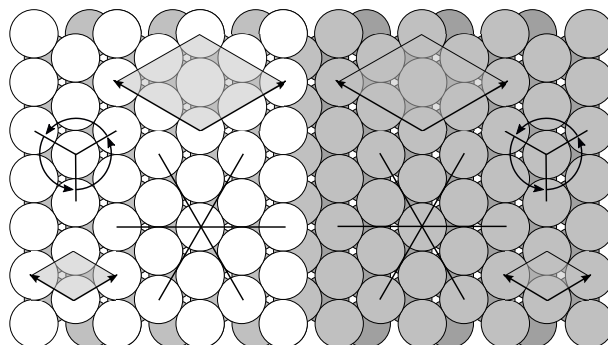


Figure 4: *Schematic view of the  $Ru\{0001\}$  surface, showing the structure either side of a single-layer step. The two-dimensional lattices (and symmetry elements) are the same on either side of the step (consistent with the  $p3m1$  space group) but the structures are mirror images of one another (aside from their height).*

From the discussion in Section 2.3, we know that reconstruction of the surface can only either retain the space group of the unreconstructed surface or transform it to a sub-group of equal or lower symmetry. Accordingly, the observation of unexpectedly higher symmetry in this case cannot be explained by reconstruction, but instead stems from a subtlety of the ideal surface. The key is to recognise that the  $\{0001\}$  surface of a hexagonal close-packed material (such as ruthenium) actually comes in two alternative forms, illustrated in Fig. 4. In this diagram, the left-hand portion shows the surface structure that we have analysed above, but the right-hand portion shows the surface structure obtained by stripping off the top layer of atoms. Evidently the structure thus exposed is identical to the original in most respects, and will actually be degenerate in terms of its energy, so for any real surface we can expect to find large terraces of both structures in equal proportion (separated by occasional atomic-height steps). Crucially, however, the structure on the right is the precise mirror image of the structure on the left, with the reflection occurring across a plane running through the step that separates them. This plane is not a mirror plane in either of the two structures themselves, each of which conforms separately to the  $p3m1$  space group within its own spatial extent.

The relevance of this state of affairs for a LEED experiment is contingent on one further piece of information, which is that the coherence length of the electrons involved is limited to around 10 nm or so. That is, the diffraction of an electron from a crystalline surface is sensitive to structural periodicity over roughly that length-scale and below, but the experiment is essentially blind to features at larger length-scales. Accordingly, if a surface displays ordered domains of spatial extent greater than around 10 nm, then a LEED experiment will yield a superposition of the diffraction patterns from all different domain types, weighted by the relative abundance of each type of domain. If the domains in question were to have entirely different reciprocal lattices, for example, then the resulting LEED pattern might not conform to either of them individually. In our case, the reciprocal lattices of both our domain types are identical, however, so the resulting LEED pattern is unchanged in terms of the diffraction spot positions. In terms of the spot intensities, on the other hand, these are obtained by mirroring the results from one domain across a plane *perpendicular* to one of the  $p3m1$  mirror planes (Fig. 3.b) and adding this to the original results. The upshot is that the summed intensities display six-fold rotational symmetry and six distinct mirror symmetries. From the LEED data alone, therefore, one might be misled into believing that the surface conforms to the  $p6mm$  space group, whereas in truth we are simply observing superposed domains that each separately conform to the  $p3m1$  space group.

Note that the behaviour described here arises intrinsically from the nature of ruthenium's bulk crystal structure (hexagonal close-packed) which contains two atoms per primitive unit cell. At the superficially similar  $\{111\}$  surface of a face-centred cubic crystal, in which the bulk primitive unit cell contains only a single atom and the layers alternate in the ...ABCABC... stacking sequence, the structure obtained by skimming off the top layer of atoms is not a mirror image of the original, and domains separated by atomic-height steps would produce identical LEED patterns, both in terms of spot positions *and* intensities. Nevertheless, it remains possible that domains related by rotational or mirror symmetry can arise upon reconstruction or adsorption. In these cases, domain superposition would not cause an apparent *increase* in symmetry relative to the ideal surface, but it is possible that it could *mask* an actual decrease in symmetry within the individual domains.

**5.2. An ARUPS experiment is performed on a Cu{111} sample (work function 4.94 eV) using light from the He I emission line (58.43 nm). What is the maximum possible surface-parallel wavevector component,  $k_{xy}$ , that can be accessed when detecting electrons emitted from 1 eV below the Fermi level? How accurately must emission angles be measured if one wishes to achieve a resolution of  $0.05 \text{ \AA}^{-1}$  in  $k_{xy}$  throughout its range for these electrons? And how would your answers change if light from the He II emission line (30.38 nm) were used instead?**

We proceed by rearranging Eqn. 5.3 from Section 5.4

$$E_b = h\nu - E_{kin} - \phi$$

to obtain

$$E_{kin} = h\nu - E_b - \phi$$

where  $h$  is the Planck constant,  $\nu$  is the frequency of the He I emission line,  $E_b$  is the binding energy of the electrons, and  $\phi$  is the work function.

We are given  $E_b = 1.00 \text{ eV}$ , and  $\phi = 4.94 \text{ eV}$ , so need only to work out the value of  $\nu$ . This we can obtain from the given wavelength ( $\lambda = 58.43 \text{ nm}$ ) since

$$\nu = c/\lambda$$

with  $c$  being the speed of light. We thus have  $\nu = (2.998 \times 10^8)/(58.43 \times 10^{-9}) = 5.131 \times 10^{15} \text{ s}^{-1}$ , and hence  $h\nu = (6.626 \times 10^{-34}) \times (5.131 \times 10^{15}) = 3.400 \times 10^{-18} \text{ J} = 21.22 \text{ eV}$ .

From this, we calculate

$$\begin{aligned} E_{kin} &= 21.22 - 1.00 - 4.94 \text{ eV} \\ &= 15.28 \text{ eV} \\ &= 2.448 \times 10^{-18} \text{ J} \end{aligned}$$

for the kinetic energy of an emitted photoelectron from 1 eV below the Fermi level.

Armed with this energy, we may now obtain the outgoing electron's wavenumber,  $k$ , by rearranging Eqn. 5.4 (from Section 5.4)

$$E_{kin} = \frac{\hbar^2 k^2}{2m_e}$$

to obtain

$$k = \sqrt{\frac{2m_e E_{kin}}{\hbar^2}}$$

where  $m_e$  is the mass of a free electron, and  $\hbar = h/2\pi$  is the reduced Planck constant.

This yields

$$\begin{aligned} k &= \sqrt{\frac{2 \times (9.019 \times 10^{-31}) \times (2.448 \times 10^{-18})}{(1.055 \times 10^{-34})^2}} \\ &= 1.992 \times 10^{10} \text{ m}^{-1} \\ &= 1.992 \text{ \AA}^{-1} \end{aligned}$$

as the wavevector of the emitted photoelectron.

Now, the surface-parallel component of the wavevector is given by Eqn. 5.5 (Section 5.4)

$$k_{xy} = k \sin \theta$$

where  $\theta$  is the emission angle relative to the surface normal. From this, it follows that the maximum possible value of  $k_{xy}$  is achieved at grazing emission, and is equal to the value of  $k$ . That is, the maximum possible value of  $k_{xy}$  in the described experiment is simply  $1.992 \text{ \AA}^{-1}$ .

Regarding resolution, it will be helpful to differentiate Eqn. 5.5, to obtain

$$\frac{dk_{xy}}{d\theta} = k \cos \theta$$

from which we deduce that the maximum rate of change in  $k_{xy}$  with respect to variation in  $\theta$  occurs at normal emission. In this worst-case scenario, we have  $d\theta = dk_{xy}/k$ , and so to be reassured that the resolution in  $k_{xy}$  will never be worse than  $0.05 \text{ \AA}^{-1}$ , we will have to ensure that we have the ability to measure angles to an accuracy no worse than  $0.05/1.992 = 0.0251 \text{ rad} = 1.44^\circ$ .

The method of calculation when using the He II emission line is identical, so will not be repeated in detail. The key intermediate values may be summarised as

$$\begin{aligned}h\nu &= 6.539 \times 10^{-18} \text{ J} = 40.82 \text{ eV} \\E_{kin} &= 34.88 \text{ eV} = 5.588 \times 10^{-18} \text{ J} \\k &= 3.009 \times 10^{10} \text{ m}^{-1} = 3.009 \text{ \AA}^{-1}\end{aligned}$$

from which we may conclude that the maximum achievable value of  $k_{xy}$  is now  $3.009 \text{ \AA}^{-1}$ , while the necessary precision in angular measurements to achieve the desired resolution in this variable becomes  $0.0166 \text{ rad} = 0.95^\circ$ . That is, use of the higher photon energy has enlarged the accessible range of reciprocal space by just over 50%, while imposing proportionally more onerous requirements upon our experimental technique if we wish to maintain the precision of our results.

**5.3. Based solely on the polarisation-dependence of the furan NEXAFS spectra depicted in Fig. 5.13, what can be said about the orientation of this molecule on the surface?**

Let us begin by noting that the data provided is specified as coming from the O 1s edge, implying two potentially important points. First, the core state involved in the integral controlling absorption (Eqn. 5.7 in Section 5.6) has spherical symmetry, which simplifies our analysis considerably. Second, whatever the nature of the unoccupied state within the integrand may be, only that portion encroaching very close to the oxygen atom of furan will be of any consequence. The latter point, it turns out, will not really change our conclusions in this particular case, but it is worth noting nonetheless, because it may not always be irrelevant.

Having recognised these points, we next notice that the two major peaks, one at around 533 eV and the other at around 540 eV, have been helpfully labelled as corresponding to  $\pi^*$  and  $\sigma^*$  orbitals of furan respectively. It will not be necessary to delve too deeply into the shapes of these orbitals, however, as the only aspect that need concern us is their symmetry with respect to the plane of the molecule. The  $\pi^*$  orbital must derive from some combination of  $p$  orbitals oriented perpendicular to the molecular plane, and so (regardless of whatever phase relationship the constituent  $p$  orbitals bear to one another) its eigenfunction must be odd with respect to reflection across the plane. The  $\sigma^*$  orbital, on the other hand, must be a combination of  $sp^2$  orbitals lying within the plane of the molecule, and its eigenfunction will therefore be even with respect to a reflection across the molecular plane.

Considering Eqn. 5.7 in more detail, then, the integrand will be an odd function for the  $\pi^*$  orbital when  $\hat{\mathbf{e}} \cdot \mathbf{r}$  is an even function with respect to the molecular plane, whilst it will be odd for the  $\sigma^*$  orbital when  $\hat{\mathbf{e}} \cdot \mathbf{r}$  is an odd function with respect to the molecular plane. Accordingly, the absorption coefficient for the  $\pi^*$  orbital will vanish when the polarisation vector lies within the plane of the molecule, while it will vanish for the  $\sigma^*$  orbital when the polarisation vector lies perpendicular to the plane of the molecule. From the graph, we see that absorption by the  $\pi^*$  orbital is minimised when the polarisation vector lies at  $90^\circ$  from the surface normal, while absorption by the  $\sigma^*$  orbital is minimised when the polarisation vector lies at  $20^\circ$  from the surface normal. We therefore conclude that the molecule must lie more-or-less flat on the surface.

It is worth noting, in passing, that the polarisation vector cannot be made to align perfectly with the surface normal, since this would require X-rays to impinge upon the surface at true grazing incidence. The  $20^\circ$  polarisation angle reported in the data will have been an experimental compromise in light of the available equipment. Presumably the peak relating to the  $\sigma^*$  orbital would have vanished more completely had a  $0^\circ$  polarisation angle been achievable. As for the  $90^\circ$  data, the disappearance of the  $\pi^*$  peak is in danger of being masked by the appearance of a peak deriving from the adsorption of residual CO (indicative of an upright species as per Fig. 5.14 in Section 5.6) but fortunately this is located at a very slightly lower photon energy and can readily be disambiguated.

**5.4. Explain why the shapes of the sticking probability and adsorption heat curves shown in Figs. 5.17 and 5.18 imply the interpretations (i.e. precursor-mediated adsorption, direct adsorption, oxidation) noted on those diagrams.**

Let us start with a descriptive summary of the data for O<sub>2</sub> adsorption. At zero coverage, the sticking probability is quite high, with a value of 0.7, but this drops fairly sharply to a value around 0.2 by the time the coverage reaches 0.2 ML. The fall is not quite fully linear, but deviations from linearity are arguably seen predominantly at the two extremes of this coverage regime. As for the heat of adsorption, this is very high to begin with, at around 630 kJ.mol<sup>-1</sup>, but falls with increasing rapidity to a little under 400 kJ.mol<sup>-1</sup> when the coverage reaches around 0.3 ML. At higher coverages, the heat of adsorption remains high, falling no lower than 350 kJ.mol<sup>-1</sup> at a coverage of over 0.7 ML and showing little indication of ever falling much further. Throughout this regime, the sticking probability remains very nearly constant, at a value of over 0.1, and although the data does not extend beyond 1 ML there is no sign of approaching saturation.

The rapidity of the initial fall in sticking probability is suggestive of direct adsorption, because it indicates that sites for fresh adsorption are being progressively blocked by adsorbates that have previously attached to the surface. The high initial heat of adsorption is typical of a dissociative process, where the intramolecular bond is sacrificed to allow much stronger binding between isolated adatoms and the metal surface. Furthermore, the accelerating (and eventually rapid) drop in adsorption heat is consistent with long-range repulsive interactions between adatoms that bind to the surface in predominantly ionic fashion. Intact molecules, binding to the surface by covalent means, would probably have comparatively weak lateral interactions. Finally, the constancy of both sticking probability and adsorption heat in the high-coverage regime indicates the onset of a surface process capable of eventually incorporating more oxygen than could reasonably be accommodated within a single layer. At surface temperatures low enough for oxygen to condense from the gas phase, it might have been possible to argue that this could, in fact, correspond to the formation of a multilayer comprising physisorbed oxygen molecules, but (a) this would not be consistent with the high heat of adsorption that is measured, and (b) we are told that the experiments were performed at room temperature. The only sensible explanation is that oxygen atoms incorporate into sub-surface sites, diffusing downwards into the material and forming an ever-thickening oxide layer.

Turning to the CO adsorption data, we see that the sticking probability is again initially quite high, with a value of over 0.7, but in contrast with the previous example it falls only relatively slowly with coverage. Indeed, the sticking probability falls below 0.6 only at a coverage around 0.5 ML, and only subsequently starts to decline in a more rapid fashion. The heat of adsorption, meanwhile, is initially fairly modest, at 140 kJ.mol<sup>-1</sup>, but remains at much the same level until the coverage exceeds around 0.4 ML. Thereafter, the adsorption heat starts to decline in a fairly linear fashion, but drops by rather less than 30 kJ.mol<sup>-1</sup> as the coverage doubles from that point.

The slow initial decline in sticking probability is consistent with a process mediated by a mobile precursor state, since arriving molecules can then roam the surface to find a suitable adsorption site even if the site at which they first arrive is already occupied. Furthermore, if adsorption involves intact molecules, repulsive lateral interactions are likely to be weak and fairly short-range in nature, allowing the heat of adsorption to remain almost constant until the coverage becomes quite high, so long as their precursor phase permits them to find their most favourable permanent adsorption site. Eventually, as empty sites start to become sufficiently scarce, both the sticking probability and adsorption heat will necessarily decline more steeply, but weak lateral interactions nevertheless imply only a relatively modest drop in the latter quantity.

**5.5. Molecular nitrogen adsorbs on a flat and featureless metal surface. Discuss whether one should expect to see absorption attributable to the N–N stretch mode in a RAIRS experiment, if either (i) the molecules bind to the surface end-on, via a single nitrogen atom each, or (ii) the molecules lie flat on the surface, binding through both of their nitrogen atoms.**

The first point to recollect is that absorption of infrared light is dependent upon the molecule's dynamic dipole moment, not on its equilibrium dipole moment (see Section 5.8). Carbon monoxide, for instance, has only a rather small gas-phase dipole moment of around 0.2 D, but a particularly large dynamic dipole moment of around  $3.0 \text{ D}/\text{\AA}$  for the C–O stretch mode (see Fig. 2 in Meshkov *et al* [*J. Quant. Spectrosc. Radiat. Transf.* **280**, 108090 (2022)] for a good illustration of this). Consequently, CO is a strong absorber of infrared light at the corresponding stretch frequency, despite being almost non-polar in its ground state.

Turning to molecular nitrogen, then, the absence of a ground-state dipole moment for this symmetric diatomic does not, in itself, disqualify it from being infrared active in the gas phase. Its high symmetry does, however, imply that its dipole moment cannot change upon variation of its bond length, which in turn implies a vanishing dynamic dipole moment and hence no gas-phase infrared absorption.

When adsorbed vertically on a metal surface, however, binding through just one of its nitrogen atoms, the symmetry of the gas-phase molecule is evidently broken. The two nitrogen atoms experience quite different local environments, and there is consequently no longer any reason to suppose that the molecule's dipole moment will be zero. More importantly, for our purpose, there is also no longer any reason to suppose that a change in bond length will fail to induce any change in dipole moment, since our original symmetry argument no longer applies. It is, of course, quite impossible to predict how large the dynamic dipole moment may be, and so the absorption may be either weak or strong depending upon details of the molecule–surface interaction. But there is no doubt that some degree of infrared absorption ought to occur.

When adsorbed horizontally, in contrast, the two nitrogen atoms experience identical local environments, just as they did in the gas phase. Moreover, the molecule retains reflection symmetry across a plane bisecting the N–N bond. Accordingly, we may deduce that there can be no dipole moment (or dynamic dipole moment) in the direction of the bond, based on the same symmetry arguments that we used in the gas phase. Importantly, however, this is actually quite irrelevant in relation to the absorption of infrared light, since the surface selection rule means that we would not expect absorption from the lateral component of a dynamic dipole moment anyway. The subtle point here is that a variation in N–N bond length of the horizontal molecule may, in fact, modify the degree of any charge transfer that occurs between the adsorbate and the substrate (because it may alter the energy of the molecule's frontier orbitals relative to the surface's Fermi level). If electrons move vertically as the molecule vibrates laterally, then this will constitute a varying dipole moment in the surface-normal direction. Once again, therefore, we should anticipate absorption of infrared light at the frequency corresponding to the N–N stretch mode.